Cong Yin, Zheng-Zhe Lin*, Min Li and Hao Tang

Understanding the Formation Mechanism of Two-Dimensional Atomic Islands on Crystal Surfaces by the Condensing Potential Model

DOI 10.1515/zna-2015-0511
Received December 7, 2015; accepted December 28, 2015; previously published online January 29, 2016

Abstract: A condensing potential (CP) model was established for predicting the geometric structure of two-dimensional (2D) atomic islands on crystal surfaces. To further verify the CP model, statistical molecular dynamics simulations are performed to investigate the trapping adatom process of atomic island steps on Pt (111). According to the detailed analysis on the adatom trapping process, the CP model should be a universal theory to understand the shape of the 2D atomic islands on crystal surfaces.

Keywords: Condensing Potential Model; Crystal Surface; Two-Dimensional Islands.

PACS Numbers: 68.35.Ja; 71.15.Pd.

1 Introduction

In thin film growth, the formation mechanism of two-dimensional (2D) islands on crystal surfaces is of great importance for fundamental research on surface science and lots of related surface technologies [1–13]. In 1901, to determine the equilibrium shape of crystal of fixed volume inside a separate phase, the famous Wulff construction based on the minimum free energy principle was proposed and now is also widely used to understand and predict the equilibrium shape of 2D islands on crystal surfaces. However, the theory is not applicable for epitaxial islands grown at temperatures lower than the ones for equilibrium growth. For instance, the Wulff construction can well understand the vacancy 2D islands of truncated triangular shapes formed by ion sputtering on Pt (111) surface at about 700 K [14–16] but cannot reproduce the exact triangular shapes of homoepitaxial 2D islands on Pt (111) surfaces at about 400 K [17].

Recent experimental and theoretical studies reveal the influence of substrate lattice orientation on the growth of 2D film [24–27]. The growth condition of 2D islands or film could be in non-equilibrium and thus beyond the prediction of the Wulff construction. In our previous work [18], a condensing potential (CP) model was first proposed to predict the shape of 2D adatom islands grown at low temperatures. For the growth of 2D islands, the CP model mainly considers two types of adatom diffusion: approaching island step and moving along island step (Fig. 1a), and predicts the shapes of 2D islands by evaluating the ability of island steps capturing wandering adatoms. The CP model has been applied successfully in several cases, including the triangular island shape on Pt (111) at 400 K. As the CP model was given with only qualitatively analysis, a quantitative explanation by statistical molecular dynamics (MD) simulations is necessary to testify the universality of the CP model.

In this work, statistical MD simulations are performed to verify the CP model applied in predicting the growth of the 2D atomic epitaxial or vacancy islands. For (100) and (111) faceted steps on the Pt (111) surface, their capturing ability to wandering adatoms is investigated. According to the result, the ability of A and B steps capturing wandering adatoms is in good agreement with the prediction of CP model. Density functional theory (DFT) calculations are employed to verify the accuracy of empirical potential used in MD. In summary, the CP model, which can be carried on simply, is reliable for the prediction of the 2D atomic island shape.

2 The CP Model

In homoepitaxial growth, the atoms deposited onto a crystal surface form small 2D clusters, which eventually grow into islands with certain shapes by capturing the landed atoms wandering on the surface. For predicting the

***Corresponding author: Zheng-Zhe Lin,** School of Physics and Optoelectronic Engineering, Xidian University, Xi'an 710071, China, E-mail: linzhengzhe@hotmail.com.
http://orcid.org/0000-0001-7188-6257
Cong Yin, Min Li and Hao Tang: Central Academy of Dongfang Electric Corporation, Chengdu 611731, China

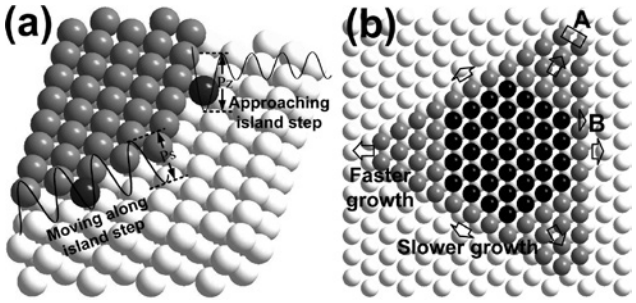

Figure 1: (a) Schematics of two ways of an adatom merging into a 2D island on a Pt (111) surface and the corresponding energy barriers. (b) On Pt (111) surface the (100) faceted A step becomes shorter in length as it grows faster with larger CP than the (111) faceted B step, leading to triangular islands surrounded by the B step.

growth of 2D islands, the CP model [18] mainly considers two types of adatom diffusion: approaching island step and moving along island step (Fig. 1a), with corresponding potential energy barriers P_z and P_s, respectively. The ability for an island step to capture a wandering adatom should increase with P_z and P_s, i.e. the larger P_z and P_s are, the more probably the wandering adatom is captured by the step. For an island step with a large P_z (or P_s) but small P_s (or P_z), the wandering atom cannot be strongly fastened. Therefore, the CP is defined as $P = P_z \times P_s$. Obviously, for an island step with a larger CP, it is more probable for the adatoms to stay stable on it, resulting in a faster growth of the step and shorter in length correspondingly (Fig. 1b).

On a Pt (111) surface, there exists two close-packed island steps: the (100) faceted A step and the (111) faceted B step (Fig. 2a and b). For the CP values of the adatom on the A and B steps, the calculations are performed by semi-empirical tight-binding (TB) potential [19]. The simulation system is modelled as an infinite A or B step with a nine-layer substrate with 12×10 Pt atoms in each layer. The surface consists of upper and lower terraces separated by a (111) microfaceted monatomic steps. Periodic boundary conditions are imposed both parallel and perpendicular to the surface. The detailed method of CP calculation can be seen in Yin et al. [18]. According to the result (Tab. 1),

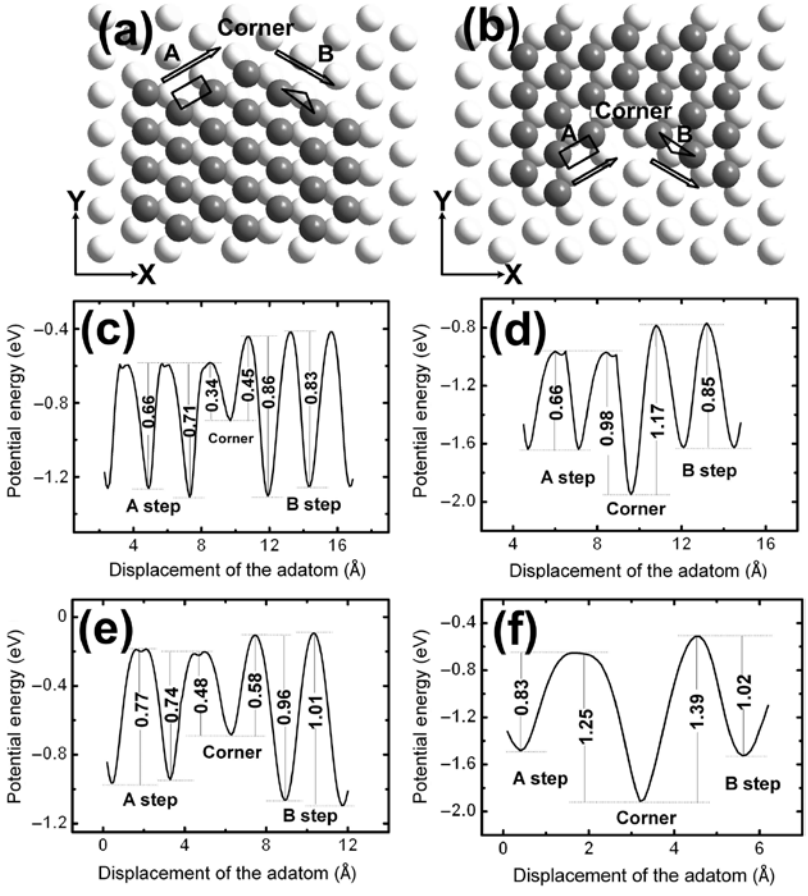

Figure 2: On the Pt (111) surface, movement of an adatom from the A step to the corner and then to the B step in an epitaxial island (a) or a vacancy island (b). Potential energy profile and energy barriers in the (a) and (b) processes calculated by TB potential (c) and (d), respectively. Potential energy profile and energy barriers in the (a) and (b) processes calculated by DFT calculations (e) and (f), respectively.

Table 1: The P_s (eV), P_z (eV) and CP (eV^2) values of the A and B steps on Pt (111) surface via TB potential and DFT calculations.

Step	TB potential			DFT		
	P_s	P_z	CP	P_s	P_z	CP
A	0.65	1.86	1.21	0.82	2.43	1.99
B	0.84	0.91	0.76	0.97	1.13	1.11

by the TB potential the CP value of A step is about 1.6 times that of B step.

3 DFT Calculation

To verify the aforementioned CP values of the adatom on the A and B step derived by TB potential, calculations are performed by DFT method. The Vienna Ab Initio Simulation Package [20] is employed. Ultrasoft pseudopotentials are used for the electron–ion interactions [21] with a cutoff energy of 191.4 eV, and the exchange-correlation effect is described by the generalised gradient approximation [22]. Periodic boundary conditions are imposed both parallel and perpendicular to the model surface. The Brillouin zone is sampled with $2\times4\times1$ k-points sampling of the Monkhorst–Pack grid [23]. The simulation system is modelled as an infinite A or B step on a four-layer Pt (111) slab with 8×5 atoms per layer. According to the result (Tab. 1), by DFT calculation the CP value of A step is about 1.8 times that of B step, which is close to the ratio 1.6 by the TB potential. So the credibility of the TB potential is verified, and the following results inferred by the TB potential can be trusted.

4 MD Simulations

Before performing MD simulations, we first examined the reliability of TB potential [19] by comparing the potential energy barriers of adatom on the island steps obtained from the TB potential with DFT calculations. For the TB potential, the system is modelled by a nine-layer substrate with 12×10 Pt atoms in each layer. Then, a Pt adatom was initially located on the surface near A step and moved along the periphery. To obtain the potential energy profile, the X coordinate of the adatom increased by 0.1 Å step by step, and at each step the system is relaxed to local energy minimum with the X coordinate of the adatom and the bottom layer of the substrate fixed. For the processes shown in Figure 2a and b, the potential energy profile and energy barriers are shown in Figure 2c and d, respectively. For DFT calculations, the system was modelled by a four-layer Pt (111) slab with 8×5 atoms per layer. The surface consists of upper and lower terraces separated by a (111) microfaceted monatomic step. Periodic boundary conditions are imposed both parallel and perpendicular to the surface. For the processes shown in Figure 2a and b, the potential energy profile and energy barriers are shown in Figure 2e and f, respectively. According to the results, the energy barriers obtained by the TB potential are all about 80 % of those by DFT calculations. Because the potential energy profiles obtained by the TB potential and DFT calculations have the same trend, we believe that the TB potential is reliable for MD calculations on the Pt (111) surface.

Then, MD simulations are performed to investigate the probability of Pt adatom captured by the A and B step. The simulation system is modelled by a nine-layer Pt (111) substrate with 15×15 atoms in each layer arranged in perfect lattices. A and B steps are structured on the substrate (Fig. 3a). An adatom is initially located on the Pt (111) terrace with the same distance h to the A step as to the B step. The periodic boundary condition is applied on the X and Y directions. The dashed line in Figure 3a shows the periodic boundary in the X direction, and thus Figure 3a actually doubles the view of the simulation system. A thermal bath at constant temperature $T=800$ K is applied on the bottom layer of the substrate. Velocity Verlet algorithm is employed with a time step of 0.2 fs. After a sufficient long time of constant-temperature MD simulation, the adatom would be captured by the A or B step, or trapped in the corner during diffusing. As soon as the adatom is captured, it is relocated at its initial position as

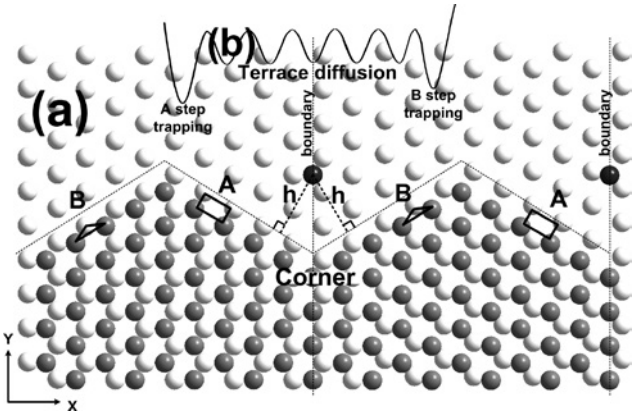

Figure 3: (a) Schematics of the MD simulation model doubling the top view of the system, with the dashed line presenting the periodic boundary in the X direction. (b) The energy barriers of the adatom on the terrace.

Table 2: The count of the adatom captured by the A step, B step, and the corner in MD simulations.

Position	$h=5$ Å	$h=8$ Å
A step	2412	1805
B step	1375	1784
Corner	592	217

the black ball shows in Figure 3. This process is repeated, and the count of the adatom captured by the A step (f_A), B step (f_B), and the corner (f_C) is recorded in Table 2.

The previous simulation is performed with the initial distance of the adatom the island step $h=5$ and 8 Å. As shown in Table 2, for $h=8$ Å $f_A/f_B=1.01$, and for $h=5$ Å $f_A/f_B=1.75$. This indicates that there should be a critical distance h_C between the freely diffusing adatom and the island step. As shown in Figure 3b, as h gets larger there is more diffusion energy barriers between the trapping potential valley of A step and that of B step. When $h>h_C$, the wandering adatom may diffuse on the terrace randomly, because the steps are quite far way. When $h<h_C$, the movement of the adatom is strongly affected by the steps, and the trapping ability for the steps dominates the diffusion of the adatom. So the value $f_A/f_B=1.75$ should be more reliable. This ratio presents the ratio of trapping ability between A and B steps.

In Table 1, we see that the CP value of the A step is about 1.59 times that of the B step by the TB potential. By DFT calculation, this proportion is about 1.81. Because this ratio of CP values is close to f_A/f_B, we suggest that the CP values of the steps thoroughly describe their atom-trapping ability. It is worth noting that the atom-trapping ability cannot be simply evaluated by the potential energy barrier P_z. By the TB potential, the proportion of P_z between A and B steps is 2.03, and by DFT calculation this value is about 2.15. The fact that the proportion of P_z between A and B steps is far away from f_A/f_B indicates that P_z cannot be used to evaluate the atom-trapping ability of the steps.

5 Conclusions

In summary, this work consolidates the reliability of the CP model in predicting the shape of 2D atomic islands on crystal surfaces. We obtained the statistical data of the adatom trapping by the island steps through huge amounts of MD simulations and proved that the CP model could actually generalise the physical processes of adatoms captured by the island steps. Thus the prediction of the 2D atomic island shape can be carried on simply and precisely by the CP model.

References

[1] J. A.Venables, Introduction to Surface and Thin Film Processes, Cambridge University Press, Cambridge, UK 2000.
[2] T. Michely, M. Kalff, G. Comsa, M. Strobel, and K. H. Heinig, Phys. Rev. Lett. **86**, 2589 (2001).
[3] M. Schmid, C. Lenauer, A. Buchsbaum, F. Wimmer, G. Rauchbauer, et al., Phys. Rev. Lett. **103**, 076101 (2009).
[4] C. Busse, H. Hansen, U. Linke, and T. Michely, Phys. Rev. Lett. **85**, 326 (2000).
[5] C. Busse, C. Polop, M. Müller, K. Albe, U. Linke, et al., Phys. Rev. Lett. **91**, 056103 (2003).
[6] S. A. Chaparro, Y. Zhang, and J. Drucker, Appl. Phys. Lett. **76**, 3534 (2000).
[7] P. J. Feibelman, Phys. Rev. B **60**, 4972 (1999).
[8] J. M. MacLeod, J. A. Lipton-Duffin, U. Lanke, S. G. Urquhart, and F. Rosei, Appl. Phys. Lett. **94**, 103109 (2010).
[9] T. Y. Fu, and T. T. Tsong, Phys. Rev. B **61**, 4511 (2000).
[10] O. Pietzsch, A. Kubetzka, M. Bode, and R. Wiesendanger, Phys. Rev. Lett. **92**, 057202 (2004).
[11] H. Brune, Surf. Sci. Rep. **31**, 125 (1998).
[12] M. M. Shen, D. J. Liu, C. J. Jenks, P. A. Thiel, and J. W. Evans, J. Chem. Phys. **130**, 094701 (2009).
[13] K. Morgenstern, E. Lægsgaard, and F. Besenbacher, Phys. Rev. Lett. **94**, 166104 (2005).
[14] T. Michely and G. Comsa, Surf. Sci. **256**, 217 (1991).
[15] D. C. Schlößer, L. K. Verheij, G. Rosenfeld, and G. Comsa, Phys. Rev. Lett. **82**, 3843 (1999).
[16] J. Ikonomov, K. Starbova, H. Ibach, and M. Giesen, Phys. Rev. B **75**, 245411 (2007).
[17] M. Kalff, G. Comsa, and T. Michely, Phys. Rev. Lett. **81**, 1255 (1998).
[18] C. Yin, X. J. Ning, J. Zhuang, Y. Q. Xie, X. F. Gong, et al., Appl. Phys. Lett. **94**, 183107 (2009).
[19] F. Cleri and V. Rosato, Phys. Rev. B **48**, 22 (1993).
[20] G. Kresse and J. Furthmüller, Phys. Rev. B **54**, 11169 (1996).
[21] D. Vanderbilt, Phys. Rev. B **41**, 7892 (1990).
[22] J. P. Perdew, J. A. Chevary, S. H. Vosko, K. A. Jackson, M. R. Pederson, et al., Phys. Rev. B **46**, 6671 (1992).
[23] H. J. Monkhorst and J. D. Pack, Phys. Rev. B **13**, 5188 (1976).
[24] J. M. Wofford, S. Nie, K. Thurmer, K. F. McCarty, and O. D. Dubon, Carbon **90**, 284 (2015).
[25] X. Chen, Y.-W. Wang, X. Liu, X.-Y. Wang, X.-B. Wang, et al., Appl. Surf. Sci. **345**, 162 (2015).
[26] D. V. Gruznev, A. V. Matetskiy, L. V. Bondarenko, O. A. Utas, A. V. Zotov, et al., Nat. Comm. **4**, 1679 (2013).
[27] D. A. Olyanich, V. V. Mararov, T. V. Utas, O. A. Utas, D. V. Gruznev, A. et al., Surf. Sci. **635**, 94 (2015).